



ARL-TR-9212 • MAY 2021



The Use of Engineering Circuit Analysis to Describe the Joule-Heating Distribution of Several Electrical-Conductivity Averaging Schemes for Mixed Computational Cells

by Steven B Segletes

Approved for public release; distribution is unlimited.

NOTICES

Disclaimers

The findings in this report are not to be construed as an official Department of the Army position unless so designated by other authorized documents.

Citation of manufacturer's or trade names does not constitute an official endorsement or approval of the use thereof.

Destroy this report when it is no longer needed. Do not return it to the originator.



The Use of Engineering Circuit Analysis to Describe the Joule-Heating Distribution of Several Electrical-Conductivity Averaging Schemes for Mixed Computational Cells

by Steven B Segletes

Weapons and Materials Research Directorate, DEVCOM Army Research Laboratory

REPORT DOCUMENTATION PAGE

Form Approved
OMB No. 0704-0188

Public reporting burden for this collection of information is estimated to average 1 hour per response, including the time for reviewing instructions, searching existing data sources, gathering and maintaining the data needed, and completing and reviewing the collection information. Send comments regarding this burden estimate or any other aspect of this collection of information, including suggestions for reducing the burden, to Department of Defense, Washington Headquarters Services, Directorate for Information Operations and Reports (0704-0188), 1215 Jefferson Davis Highway, Suite 1204, Arlington, VA 22202-4302. Respondents should be aware that notwithstanding any other provision of law, no person shall be subject to any penalty for failing to comply with a collection of information if it does not display a currently valid OMB control number.

PLEASE DO NOT RETURN YOUR FORM TO THE ABOVE ADDRESS.

1. REPORT DATE (DD-MM-YYYY) May 2021		2. REPORT TYPE Technical Report		3. DATES COVERED (From - To) February 2021–May 2021	
4. TITLE AND SUBTITLE The Use of Engineering Circuit Analysis to Describe the Joule-Heating Distribution of Several Electrical-Conductivity Averaging Schemes for Mixed Computational Cells				5a. CONTRACT NUMBER	
				5b. GRANT NUMBER	
				5c. PROGRAM ELEMENT NUMBER	
6. AUTHOR(S) Steven B Segletes				5d. PROJECT NUMBER	
				5e. TASK NUMBER	
				5f. WORK UNIT NUMBER	
7. PERFORMING ORGANIZATION NAME(S) AND ADDRESS(ES) DEVCOM Army Research Laboratory ATTN: FCDD-RLW-TC Aberdeen Proving Ground, MD 21005-5066				8. PERFORMING ORGANIZATION REPORT NUMBER ARL-TR-9212	
9. SPONSORING/MONITORING AGENCY NAME(S) AND ADDRESS(ES)				10. SPONSOR/MONITOR'S ACRONYM(S)	
				11. SPONSOR/MONITOR'S REPORT NUMBER(S)	
12. DISTRIBUTION/AVAILABILITY STATEMENT Approved for public release; distribution is unlimited.					
13. SUPPLEMENTARY NOTES author's email: <steven.b.segletes.civ@mail.mil>.					
14. ABSTRACT The use of the electrical circuit diagram is put forward as a useful tool for understanding the behavior and consistency of electrical conductivity averaging schemes for mixed-cell computations. Sub-circuits are developed for each of three separate conductivity-averaging schemes: volume averaged, harmonic averaged, and the conductivity model of ARL-TR-8979. The circuit component properties derive from properties of the mixed cell, such as species conductivity and volume fraction. These sub-circuits are shown to produce the proper values of net conductivity espoused by the respective models. Once proper conductivity behavior has been verified, engineering analysis is performed on the circuit to determine the joule-heating distribution among the various species of the mixed cell. A richer understanding emerges of the conductivity-averaging schemes with respect to their behavior as species volume fractions vary. Spreadsheet tools are developed to exercise and play test various mixed-cell scenarios.					
15. SUBJECT TERMS conductivity, joule heating, mixed cell, averaging scheme, magnetohydrodynamics, circuit analysis					
16. SECURITY CLASSIFICATION OF:			17. LIMITATION OF ABSTRACT UU	18. NUMBER OF PAGES 38	19a. NAME OF RESPONSIBLE PERSON Steven B Segletes
a. REPORT Unclassified	b. ABSTRACT Unclassified	c. THIS PAGE Unclassified			19b. TELEPHONE NUMBER (Include area code) 410-278-6010

Contents

List of Figures	iv
List of Tables	v
Acknowledgments	vi
1. Introduction	1
2. Volume-Average Approach to Conductivity	1
3. Harmonic-Average Approach to Conductivity	4
4. Equivalent Circuit for the Conductivity Model of ARL-TR-8979	6
5. Verification Results and Other Comparisons	11
5.1 Verification of Equivalent Circuit to Model of ARL-TR-8979	12
5.2 Example: Balanced Species Distribution	15
5.3 Example: Predominant Greater-Conducting Component	18
5.4 Example: Predominant Lesser-Conducting Component	20
5.5 Overall Comparison of the Conductivity-Averaging Schemes	22
5.5.1 Conductivity	22
5.5.2 Joule Heating	22
6. Possible Inconsistencies for Further Study	24
7. Conclusion	25
8. References	28
Distribution List	29

List of Figures

- Fig. 1 The a) schematic and b) resulting sub-circuit associated with treating a mixed computational cell with the volume-averaged approach2
- Fig. 2 The a) schematic and b) resulting sub-circuit associated with treating a mixed computational cell with the harmonic-averaged approach.....4
- Fig. 3 A schematic visualizing conduction through a mixed cell of three materials, in which the constituent species are ordered to satisfy the relation $\kappa_1 > \kappa_2 > \kappa_3$. This model, when generalized for n components, can be shown equivalent to that described in ARL-TR-8979.7
- Fig. 4 The equivalent circuit used to describe a mixed cell of three materials, according to the model of ARL-TR-8979. The first index of the resistance denotes the electrical channel on which the resistor lies and the second index the material species composing the resistor.8
- Fig. 5 Probability F of establishing connectivity across the diagonal of various 3-D cubic network cascades, as a function of f , the likelihood that any given network link is conductive. Originally Fig. 2 of ARL-MR-1030.⁵ 10

List of Tables

Table 1	Example mixed cell to demonstrate the effect of conductive uniformity (originally Table A-1b of ARL-TR-8979)	12
Table 2	Net conductivity when conductively uniform species (2 and 3) combine pathways (originally Table A-3 of ARL-TR-8979; equation numbers refer to ARL-TR-8979).....	12
Table 3	Spreadsheet solving equivalent mixed-cell circuit, showing compatibility with result presented in Appendix A of ARL-TR-8979.....	13
Table 4	Summary of results presented in Table 3	15
Table 5	The $F(f)$ function used for subsequent examples, corresponding to a $5 \times 5 \times 5$ cubic 3-D lattice.....	16
Table 6	Summary of results presented in Table 7	16
Table 7	Equivalent mixed-cell circuit, with $\kappa_1 = 1$ (33%), $\kappa_2 = 0.1$ (34%), and $\kappa_3 = 0.01$ (33%).....	17
Table 8	Summary of results presented in Table 9	18
Table 9	Equivalent mixed-cell circuit, with $\kappa_1 = 1$ (75%), $\kappa_2 = 0.1$ (10%), and $\kappa_3 = 0.01$ (15%).....	19
Table 10	Summary of results presented in Table 11.....	20
Table 11	Equivalent mixed-cell circuit, with $\kappa_1 = 1$ (15%), $\kappa_2 = 0.1$ (10%), and $\kappa_3 = 0.01$ (75%).....	21

Acknowledgments

The author is very grateful to Dr Paul Berning who conducted a useful technical review of the work. It is perhaps even prior conversations with Dr Berning that initially put the idea into the author's mind to treat the mixed cell as an equivalent circuit. The author is again indebted to Ms Carol Johnson, for her most excellent editorial review work that she brings to bear on any manuscript, including this one.

1. Introduction

In ARL-TR-8979,¹ the author proposed a model for the electrical-conductivity averaging of a mixed computational cell, assuming randomly distributed material species of given volume-fraction at a specified minimum granularity.

In this report, we intend to accomplish two goals: to re-express the models of ARL-TR-8979 and several others in a fashion that can be laid out as engineering circuit diagrams that may prove a better mnemonic for understanding the original derivations; and extend the results, so as to calculate the joule heating in the cell according to the respective averaging scheme, including the total power as well as the partition of the power deposition into each of the mixed-cell component species.

2. Volume-Average Approach to Conductivity

In engineering treatments of electrical circuits, the electrical *component* is the smallest unit considered therein. Electrical behavior within the component is idealized. Nonideal gradients and inhomogeneities within the component are not considered. In the case of the idealized resistor (of interest in this report’s treatment), the electric field and current flow are constant and the voltage varies linearly along the direction of current flow.

While the electrical treatment within a magnetohydrodynamics (MHD) code can macroscopically treat current flow in a “continuum”, at a small enough scale—the level of the computational cell—the treatment reaches component level and electrical properties are idealized therein. A problem of poor accuracy arises when this smallest component, the computational cell, contains several different material species of vastly different electrical properties. The challenge is to formulate an appropriate sub-circuit within this component we call the computational cell.

The standard approach, which does not always work well to describe electrical behavior, is that of volume averaging, in which the aggregate conductivity of the mixed cell is described as

$$\kappa_a = \sum_{j=1}^n \kappa_j v_j \quad . \quad (1)$$

Here, κ is the electrical conductivity and v_j is the volume fraction of material species j in the cell containing n separate material species. The subscript “a” refers

specifically to the volume-averaged approach discussed in this section.

We will find it extremely helpful, in both understanding and analysis, to describe the mixed-cell averaging scheme as an explicit electrical sub-circuit, since the engineering approach to analyze circuits is well established. For purposes of illustration, we consider a mixed cell containing three species. We now show that the schematic and the resulting sub-circuit, shown in Fig. 1, are representative of the volume-averaging approximation.

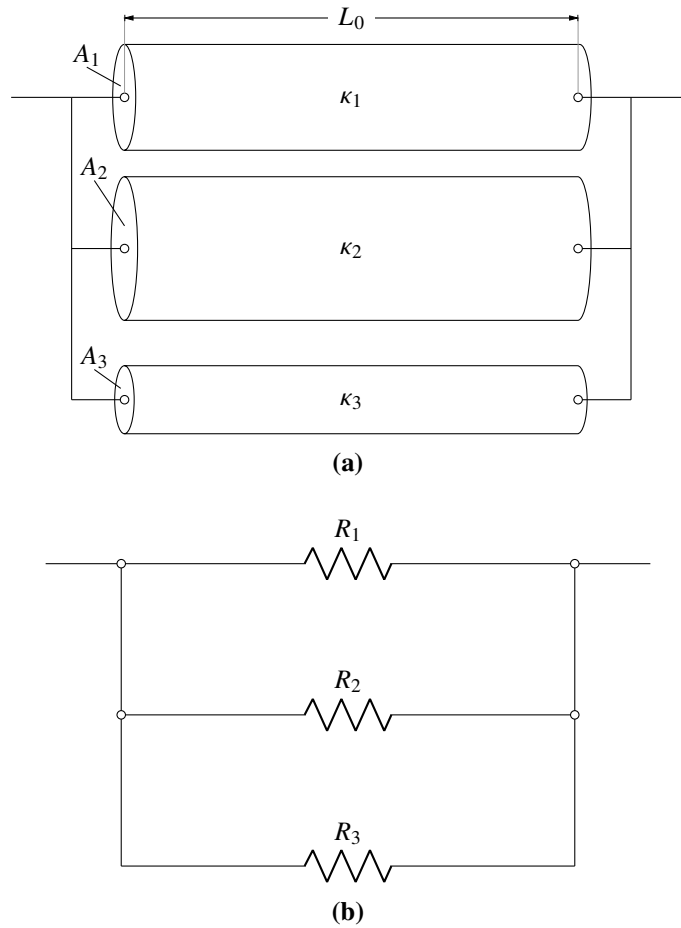


Fig. 1 The a) schematic and b) resulting sub-circuit associated with treating a mixed computational cell with the volume-averaged approach

In the schematic, the length L_0 is the total length of the cell in the direction of the local electric field, and the total area, $A_0 = A_1 + A_2 + A_3$, is the cell's cross section perpendicular to the local electric field. The areas shown are proportioned such that $A_j L_0$ represents the total volume of the mixed-cell species j in that cell. The fraction A_j/A_0 is, therefore, the volume fraction of species j , which we may call v_j .

To convert to the equivalent sub-circuit, we employ, for each component k of the sub-circuit, the definitions of conductance G :

$$G_k = \frac{\kappa_k A_k}{L_k} \quad (2)$$

and resistance R :

$$R_k = \frac{1}{G_k} = \frac{L_k}{\kappa_k A_k} \quad . \quad (3)$$

In this particular sub-circuit, we observe that the circuit component number signifies the material species ($k = j$) and that $L_j \equiv L_0$. Because the sub-circuit is parallel, the total conductance is the sum of the component conductances, expressed as $G_0 = \sum_{j=1}^n G_j$, which, in turn, can be expressed as $G_0 = A_0/L_0 \cdot \sum_{j=1}^n \kappa_j v_j$. But we know that $G_0 L_0/A_0$ defines the overall cell conductivity, κ_0 . We can therefore conclude that the net conductivity for the mixed-cell circuit, corresponding to our schematic idealization, is

$$\kappa_0 = \sum_{j=1}^n \kappa_j v_j \quad , \quad (4)$$

in agreement with the volume-averaged approximation of Eq. 1.

In the MHD code (continuum-approximation) setting, the power dissipated over the volume Ω_j of material j , resulting in joule heating, is given as

$$P_j = \int_{\Omega_j} \kappa_j \mathbf{E} \cdot \mathbf{E} d\Omega_j \quad . \quad (5)$$

In an idealized 1-D resistor (as in an idealized mixed cell), the magnitude of the electric field, E , will be fixed, equal to the drop in voltage per unit length, or $E = \mathcal{V}/L$. Substituting into the integral, knowing that $\int_{\Omega_j} d\Omega_j/L_j^2 = A_j/L_j$, we may eventually conclude (using Eq. 3) that

$$P_j = \mathcal{V}_j^2/R_j \quad (\text{no sum}), \quad (6)$$

the textbook equation for power loss through a resistor. Thus, we see that the continuum approach for treating the electrical response of a mixed cell is conceptually compatible with the notion of an equivalent electrical circuit that we pursue here, in terms of net conductivity and joule heating.

The total joule heating, over the complete mixed cell, is taken as²

$$P = \int_{\Omega} \kappa_0 \mathbf{E} \cdot \mathbf{E} d\Omega \quad (7)$$

While Eqs. 5 and 7 apply in all cases, in the context of Eq. 4, noting that $v_j = \Omega_j/\Omega$, we may conclude that Eq. 7 is just a statement asserting, for this volume-averaged mixed cell, that $P_a = \sum_j P_j$. Such a result is not only the logical conclusion, but also in agreement with the volume-averaged equivalent sub-circuit of Fig. 1.

Thus, the fraction of joule heating associated with component j of the mixed-cell parallel (volume-averaged) sub-circuit is

$$P_j/P_a = v_j \cdot \kappa_j/\kappa_a \quad (\text{no sum}). \quad (8)$$

In the parallel circuit, it is the most-conductive element that receives a disproportionate amount of joule heating per unit volume.

3. Harmonic-Average Approach to Conductivity

In a recent communication,³ Seifert of the ALEGRA team related alternative approaches to mixed-cell conductivity being considered at Sandia National Laboratories. One such approach was called the “harmonic average” approach, in which

$$\kappa_h^{-1} = \sum_{j=1}^n v_j \kappa_j^{-1} \quad (9)$$

The “h” subscript refers specifically to the harmonic-average approach discussed in this report section. It can be shown that this scheme is equivalent to treating the mixed cell as a serial circuit of its constituent species, as shown in Fig. 2.

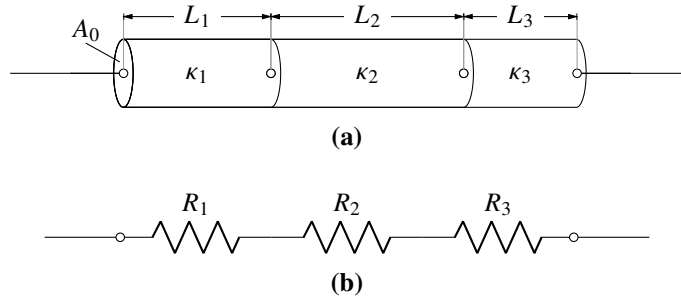


Fig. 2 The a) schematic and b) resulting sub-circuit associated with treating a mixed computational cell with the harmonic-averaged approach

Once again, the number of the circuit component k equals the material species j . Here, the length of the mixed cell is $L_0 = L_1 + L_2 + L_3$ and all species occupy the full cross section A_0 of the cell. To accurately reflect the volumes of the species of the cell, the lengths of the elements are varied so that $L_j = \Omega_j/A_0$ and $v_j = \Omega_j/\Omega = L_j/L_0$.

In a serial arrangement, the total resistance is $R_0 = \sum_{j=1}^n R_j$, which, in this case, is

$$R_0 = 1/A_0 \sum_{j=1}^n L_j/\kappa_j = L_0/A_0 \sum_{j=1}^n v_j \kappa_j^{-1} \quad ,$$

leading directly to the result that confirms Eq. 9:

$$\kappa_0^{-1} = R_0 \cdot A_0/L_0 = \sum_{j=1}^n v_j \kappa_j^{-1} \quad . \quad (10)$$

The joule heating for the harmonic-averaged mixed cell is still governed by Eq. 7, except in this case, κ_0 is governed by Eq. 10 instead of Eq. 4.

From the mixed-cell sub-circuit, the joule-heating distribution among the various material species follows the known theory for serial resistive circuits. Namely, since $P = \mathcal{V}^2/R = i^2 R$, where i is the current through the resistance, the joule heating in each component is proportional to its resistance R_j (since all serial elements transmit the same current i). This $P_j \propto R_j$ relation for the harmonic circuit may be equivalently stated as

$$P_j/P_h = v_j \cdot \kappa_h/\kappa_j \quad (\text{no sum}). \quad (11)$$

Contrast this with the volume-averaged alternative, Eq. 8, in which the joule heating is proportional to the conductivity of each resistive constituent, rather than its inverse. In the harmonic (serial) circuit, it is the least-conductive species in the series that gets the disproportionate amount of joule heating per unit volume.

4. Equivalent Circuit for the Conductivity Model of ARL-TR-8979

In ARL-TR-8979,¹ a model was proposed for the electrical-conductivity averaging in mixed computational cells. It was expressed mathematically as

$$\kappa_{1\cap\dots\cap j} = \frac{\sum_{i=1}^j v_i}{\sum_{i=1}^j \frac{v_i}{\kappa_i}} \quad , \quad \text{ARL-TR-8979: (Eq. 4)}$$

$$F_{1\cap\dots\cap j} = F_{1\cup\dots\cup j} - F_{1\cup\dots\cup j-1} \quad , \quad \text{(Eq. 5)}$$

$$F_{1\cup\dots\cup j} = F\left(\sum_{i=1}^j v_i\right) \quad , \quad \text{(Eq. 6)}$$

$$\kappa = \kappa_{1\cup\dots\cup n} = \sum_{j=1}^n F_{1\cap\dots\cap j} \kappa_{1\cap\dots\cap j} \quad . \quad \text{(Eq. 7)}$$

The notation is, perhaps, a bit obtuse for the reader—one reason why we revisit the topic in this report. Rather than trying to re-explain the notation, a summary of the key model points will suffice in its stead.

The model is based on the idea that, to the extent possible, electrical pathways (think of them as conductive filaments) will attempt to establish themselves, preferably through the most-conductive material(s). A key facet of the model is that the mixed-cell materials are assumed to be randomly distributed throughout the cell in discrete chunks no smaller than a certain assumed minimum granularity. Only when no additional pathways are available through the optimal circuit channel will less-optimal pathways be employed to carry current through the mixed cell.

The model envisions groups of electrical pathways across the mixed cell, denoting different levels of electrical preference. Such groups, which we call “pathway channels” or, simply, *channels*, are characterized by which materials they contain. All pathways within a given channel are assumed to be electrically indistinguishable. For a mixed cell of n materials, the model envisions n unique channels of conduction.

The most-preferable 1-channel is that composed solely of the most-conductive material in the cell, of conductivity κ_1 , where the materials are designated according to the rule $\kappa_1 > \kappa_2 > \dots > \kappa_n$. A statistical model, $F(v_1)$, is used to calculate the likelihood of establishing pathways that constitute the 1-channel. In general, F is a function of the volume fractions v_j of materials j composing the channel i .

When the 1-channel is exhausted, 1 \cap 2 pathways (*i.e.*, comprising materials 1 and 2) that collectively make up the 2-channel become the next most-preferable route. The F function is again employed to determine the availability of such pathways, given the larger volume fraction, $v_1 + v_2$, with which to comprise conductive paths across the mixed cell. When this channel is exhausted, 1 \cap 2 \cap 3 pathways are sought.

For our sample problem involving three species of material in the mixed cell, those are the three channels, since, if all materials are available, a connective pathway can always be found between any two arbitrary points. We are now ready to reveal the equivalent mixed-cell sub-circuit corresponding to this model in Figs. 3 and 4, for the case of $n = 3$ materials.

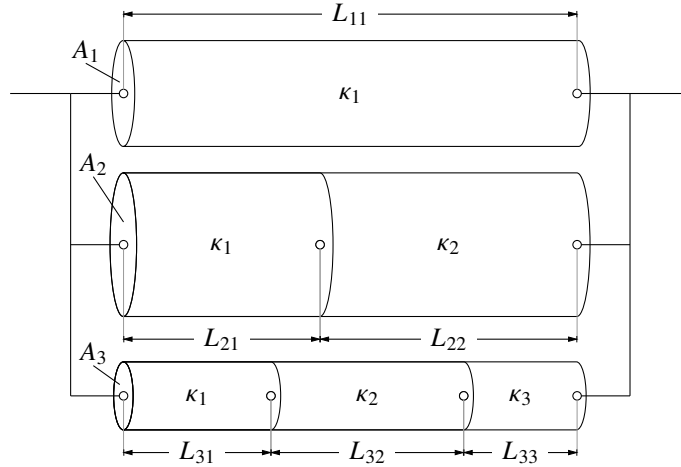


Fig. 3 A schematic visualizing conduction through a mixed cell of three materials, in which the constituent species are ordered to satisfy the relation $\kappa_1 > \kappa_2 > \kappa_3$. This model, when generalized for n components, can be shown equivalent to that described in ARL-TR-8979.

Here, for each circuit component k , we introduce a dual-index ij to help identify its unique characteristics. All that is required to fully characterize this sub-circuit is to define the meanings of κ_j , L_{ij} , and A_i in the context of the model, so that the resistances R_{ij} may be calculated according to Eq. 3. First, we use the convention that i refers to the channel number and j to the material species number in the mixed cell. The conductivity κ_j is, as we expect, the conductivity of species j , where the j are ordered so that $\kappa_1 > \kappa_2 > \kappa_3$.

For a given channel i composed of materials $j = 1, 2, \dots, i$, the likelihood of traversing a given material species is in proportion to its volume fraction among the species making up the pathways of that channel. Thus, L_{ij} , the pathlength of material j

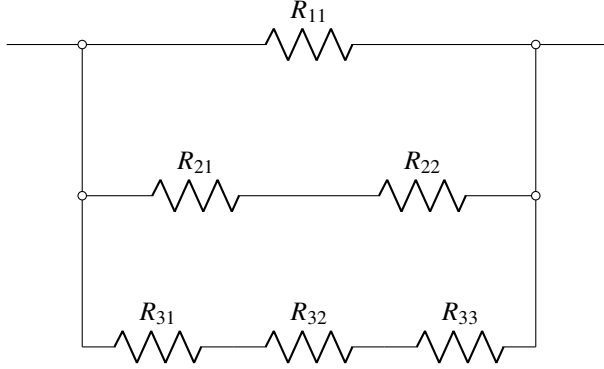


Fig. 4 The equivalent circuit used to describe a mixed cell of three materials, according to the model of ARL-TR-8979. The first index of the resistance denotes the electrical channel on which the resistor lies and the second index the material species composing the resistor.

along channel i , is

$$\frac{L_{ij}}{L_0} = \frac{v_j}{\sum_{k=1}^i v_k} . \quad (12)$$

So, for example, $L_{21}/L_0 = v_1/(v_1 + v_2)$ and $L_{32}/L_0 = v_2/(v_1 + v_2 + v_3)$. The first index of L_{ij} indicates the number of terms in the denominator and the second index the term of the numerator. The sum of the pathlengths along each of the $n = 3$ channels equals L_0 , the length of the mixed cell in the direction of the electric field.

Channel 3 of the present model is, in large regard, identical to the serial pathway of the harmonic-average circuit, with one significant difference. In the harmonic average, this constitutes the whole of the sub-circuit and all pathways conform to that makeup. Here, in contrast, only that fraction of pathways that cannot be exclusively established with species 1 and 2 will behave as a three-species serial channel.

To understand the cross-sectional areas A_i of the present model is the most challenging concept to grasp. The unique feature to understand in this model is that the material constituting each of the three channels of the sub-circuit is not isolated from the other channels. The material species 1 that makes up the sole material along the preferred channel 1 at the top of schematic Fig. 3 also participates in the transmission of current in channels 2 and 3. *Different channels can share the same physical material.* For this reason, the volume fraction of material 1 in the sub-circuit will exceed its actual volume fraction in the mixed cell. This merely means that species 1 is being over-utilized to build multiple pathways across the cell at the expense of the other species' utilization rates.

The physical meaning of A_1 in the model can be understood by considering the mixed cell if materials 2 through n could suddenly evaporate from the cell. The area $A_1/A_0 = F(v_1)$ represents the cross-sectional fraction of the cell face that is expected to electrically connect to the far end of the now partially vacant cell. Likewise, $(A_1+A_2)/A_0 = F(v_1+v_2)$ represents the cross-sectional fraction of the cell face that is expected to electrically connect if materials 3 through n were evaporated from the cell. Obviously, by the time the last (lowest conductivity) material in the cell is considered, $(A_1 + A_2 + \dots + A_n)/A_0 = F(v_1 + v_2 + \dots + v_n) = 1$ guarantees that the sum of the channel areas will equal the cross section of the cell, A_0 , and that a pathway across the cell is assured. In summary, the n equations, for $i = 1, \dots, n$, provided by

$$\frac{\sum_{k=1}^i A_k}{A_0} = F(\sum_{j=1}^i v_j) \quad , \quad (13)$$

are sufficient to determine the n values associated with A_i . Therefore, with knowledge of the κ_j conductivities in the mixed cell, along with Eqs. 12 and 13 to calculate L_{ij} and A_i , respectively, the sub-circuit representing the mixed cell is fully determined, by way of Eq. 3, as

$$R_{ij} = \frac{L_{ij}}{\kappa_j A_i} \quad (\text{no sum}). \quad (14)$$

The F function in Eq. 13 is a probabilistic function originally developed in ARL-TR-8899.⁴ There, a mixed cell of conducting and insulating material was metaphorically modeled as an $m \times m$ 2-D square network, where each linkage of the network represents a given finite volume of either conductor or insulator. A 2-D $m \times m$ nodal grid has $2m(m-1)$ linkages, and thus, each linkage represents $1/[2m(m-1)]$ of the total cell volume over which the available conductor and insulator could be randomly spread (for example, a 4×4 network has 24 linkages and thus a granularity of 4.2%). A statistical analysis is performed to determine F , the likelihood of point-to-point connectivity across the network (cell), given an expected fraction of conducting material.

Most recently,⁵ the analysis was extended to 3-D $m \times m \times m$ nodal grids, containing $3m^2(m-1)$ linkages (a $5 \times 5 \times 5$ network has 300 linkages, making a granularity of 0.33%). The particular shape of the F function will vary with the network chosen to metaphorically represent the mixed cell. However, they all share the common property of being S-shaped, because the connectivity across the network exhibits threshold behavior. The more finely granulated the network, the sharper the

threshold. Furthermore, the $F(f)$ curves are all monotonic, and possess endpoints $(0, 0)$ and $(1, 1)$. Figure 5 gives examples of F -curves for 3-D networks.

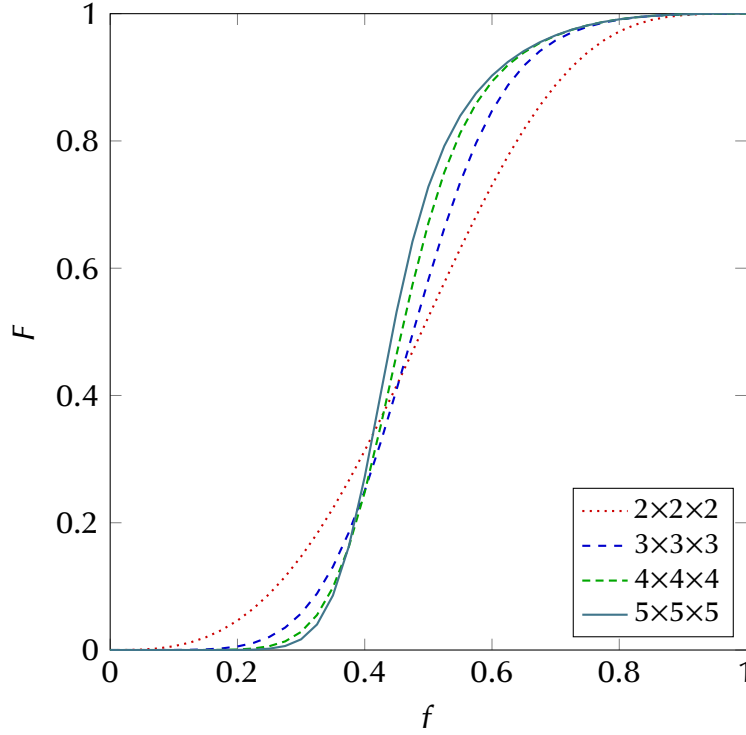


Fig. 5 Probability F of establishing connectivity across the diagonal of various 3-D cubic network cascades, as a function of f , the likelihood that any given network link is conductive. Originally Fig. 2 of ARL-MR-1030.⁵

Once all the component resistances R_{ij} are evaluated from Eq. 14 using the known or calculable values of κ_j , L_{ij} , and A_i , the sub-circuit's properties of total resistance R_0 and conductance G_0 may be calculated using undergraduate circuit-analysis techniques, arriving at

$$1/R_0 = G_0 = \sum_{i=1}^n \frac{1}{\sum_{j=1}^i R_{ij}} \quad . \quad (15)$$

The inner sum covers the components in channel i , with the outer sum covering all the channels. With those quantities in hand, the net conductivity for the mixed cell may be obtained as

$$\kappa_0 = \frac{L_0}{A_0} \sum_{i=1}^n \frac{1}{\sum_{k=1}^i R_{ik}} \quad . \quad (16)$$

The power dissipation in component ij , normalized by the square of the voltage, \mathcal{V} ,

across the cell is

$$\frac{P_{ij}}{\mathcal{V}^2} = \frac{R_{ij}}{R_i^2} = \frac{R_{ij}}{(\sum_{k=1}^i R_{ik})^2} , \quad (17)$$

where R_i is the resistance along channel i in which component ij sits.

Finally, the power dissipation (joule heating) in species j , designated $P_{.j}$, can be obtained from Eq. 17 by summing across those cross-channel components comprising species j :

$$\frac{P_{.j}}{\Omega E^2} = \frac{L_0}{A_0} \sum_{i=j}^n \frac{P_{ij}}{\mathcal{V}^2} . \quad (18)$$

We show later in this document (via spreadsheet) that the sum of these power dissipations across all species, given by $P_0/(\Omega E^2) = \sum_{j=1}^n P_{.j}/(\Omega E^2)$, yields a value identical to κ_0 (Eq. 16), which is as it should be, in accordance with Eq. 7.

In all of these calculations, extrinsic quantities like R_{ij} , R_0 , G_{ij} , and G_0 have values that vary with the scale of the mixed cell. However, the actual intrinsic quantities of interest, such as κ_0 and $P_{.j}/(\Omega E^2)$, are independent of the cell size and so dimensional quantities like L_0 and A_0 can be taken as unity if it is only the intrinsic quantities being extracted.

5. Verification Results and Other Comparisons

In considering the solution of the sub-circuit conductance, Eq. 15, one might merely be reminded that, in a serial network, resistances add, and in a parallel network, conductances add. Further, the results of ARL-TR-8979¹ still apply and may be employed for quantitative calculation as an alternate implementation.

To express the present calculations in a more tangible fashion, we share the results of a spreadsheet developed to tabulate the circuit solution and compare to the published results in ARL-TR-8979. A match, to five significant digits, between the results of the spreadsheet and the previously published report establishes equivalence between that model and the circuit depicted in Figs. 3 and 4.

Following the verification, we employ the more recently derived 5×5×5 cubic network metaphor for the mixed cell, rather than the 4×4 square network. We study cases highlighting circuit behavior when the mixed cell contains trace impurities and compare the results of the present model to that of volume averaging and harmonic averaging (*i.e.*, the parallel and serial circuit equivalents).

5.1 Verification of Equivalent Circuit to Model of ARL-TR-8979

To begin the verification, we reiterate the case we wish to verify, originally presented in the Appendix of ARL-TR-8979. While the problem contained nominally four materials, two of them (materials 2 and 3) were of identical properties, and so the analysis was conducted lumping those two together as a single “material” constituent in the cell. The volume-fraction and species-conductivity inputs are provided in Table 1 and the output in Table 2, showing the net conductivity of the mixed cell as 0.84361, using the equations of ARL-TR-8979, also reproduced at the beginning of Section 4 of this report.

Table 1 Example mixed cell to demonstrate the effect of conductive uniformity (originally Table A-1b of ARL-TR-8979)

i	v_i	κ_i
1	0.4	1.0
2 \cup 3	0.4	0.8
4	0.2	0.1

Table 2 Net conductivity when conductively uniform species (2 and 3) combine pathways (originally Table A-3 of ARL-TR-8979; equation numbers refer to ARL-TR-8979)

j	$\sum_{i=1}^j v_i$	$F_{1\cup\dots\cup j}$ Eq. 6	$F_{1\cap\dots\cap j}$ Eq. 5	$\kappa_{1\cap\dots\cap j}$ Eq. 4	$\kappa_{1\cup\dots\cup j}$ Eq. 7
1	0.40000	0.02345	0.02345	1.00000	0.02345
2 \cup 3	0.80000	0.91198	0.88853	0.88889	0.81326
4	1.00000	1.00000	0.08802	0.34483	0.84361

A spreadsheet was developed to solve the circuit described in Figs. 3 and 4, in which the above inputs were entered from Table 1. In the spreadsheet, the inputs are highlighted in bright yellow. The central columns of the spreadsheet are divided based on material species j , while the central rows are divided based on pathway channel i . The spreadsheet is replicated in Table 3.

The red numbers near the input section of the spreadsheet are values of $F(f)$ interpolated from a spreadsheet data set not shown in Table 3. They represent the functional values associated with the cumulative volume fraction of materials found along channel i of the circuit, $f = \sum_{j=1}^i v_j$. For the verification, the same F interpolation was used as that in ARL-TR-8979, namely, a 2-D 4 \times 4 square network. The tabulated $F(f)$ function can be found in Table 13 from ARL-TR-8899.

Table 3 Spreadsheet solving equivalent mixed-cell circuit, showing compatibility with result presented in Appendix A of ARL-TR-8979

INPUTS		Material 1 (is part of Paths 1,2,3)	Material 2 (is part of Paths 2,3)	Material 3 (is part of Path 3)	per Channel Aggregate	Network Aggregate
k_j	1	0.8	0.8	0.1		
v_j	0.4	0.4	0.4	0.2		
$F = \sum v_j$	0.4	0.8	0.8	1		
$F(f)^*$	0.02	0.91	0.91	1.00		
Ref: ARL-TR-8979						
Eq6 A_0	$i=$ Channel	$j=$ Circuit component composed of Mat j				
\downarrow	\downarrow	$j \rightarrow$				
$F(f)$	$A = L_i$	$k_{ij}=k_j$ $A_{ij}=A_i$ L_{ij} R_{ij} G_{ij} V_{ij}/V P_{ij}/V^2	$k_{ij}=k_j$ $A_{ij}=A_i$ L_{ij} R_{ij} G_{ij} V_{ij}/V P_{ij}/V^2	$k_{ij}=k_j$ $A_{ij}=A_i$ L_{ij} R_{ij} G_{ij} V_{ij}/V P_{ij}/V^2	R_i G_i $k_i =$	Eq 4 \downarrow ΣG_i $\Sigma G_i L_i/A_0$
0.02345	0.02345	1 42.64 0.02345 1 0.02345	2 2	3 3	42.6396 0.02345	1 0.02345 0.02345
0.91198	0.88853	1 0.88853 0.5 0.5627 1.77706 0.4 0.35102	(22)		1.26614 0.7898 0.88889	0.81326 0.81326
1	0.08802	1 0.08802 0.4 4.5446 0.22004 0.1 0.00419	(32)	(33)	G_0 $k_0 = G_0 L_0/A_0$	0.84361 0.84361
$A_0 \rightarrow$	1	$\leftarrow L_0$	\leftarrow Extrinsic totals will change with specification of overall mixed cell volume, but highlighted output does not			R_0
$\int d\Omega \rightarrow$	1	$\leftarrow E/V$ (Electric field strength/Volt = $1/L_0$)				1.18538 $G_0 = 1/R_0$ (check) 0.84361
per Material Aggregate		Power $P_{(i=2)}/(\Omega E^2)$	Power $P_{(i=2)}/(\Omega E^2)$	Power $P_{(i=3)}/(\Omega E^2)$	Power $P_{(i=2)}$	Conductivity
joule heating (per Ω):		0.37866 % Mat 1	0.44401 % Mat 2	0.02093 % Mat 3	0.84361 \leftarrow ARL-TR-8979 \rightarrow	$k_0 =$ 0.84361
volume average compare		$v_1 k_1$ 0.4 % Mat 1 54.05%	$v_2 k_2$ 0.32 % Mat 2 43.24%	$v_3 k_3$ 0.02 % Mat 3 2.70%	$\Sigma_j v_j k_j$	$\Sigma_j v_j k_j$
harmonic average compare		$v_1 k_0^2/k_1$ 0.04756 % Mat 1 13.79%	$v_2 k_0^2/k_2$ 0.05945 % Mat 2 17.24%	$v_3 k_0^2/k_3$ 0.23781 % Mat 3 68.97%	0.74 \leftarrow Volume Avg \rightarrow $\Sigma_j v_j k_0^2/k_j$	$k_0 =$ 0.74 $1/(\Sigma_j v_j/k_j)$
					0.34483 \leftarrow Harmonic Avg \rightarrow	$k_0 =$ 0.34483

* Excelis interpolating F(f) from the chart off the right, it is the 4x4 S-curve (This example is Tables A-1(b) and A-3 of ARL-TR-8979)

The cross section A_0 and cell length L_0 of the mixed cell, highlighted in a pale yellow, can be exercised as inputs, if desired. Doing so will change extrinsic properties of the circuit such as resistance and conductance. However, the intrinsic properties of interest, such as net conductivity and joule heating per unit volume, will be unaffected by any changes to the dimensions of the mixed cell.

Four columns to note (two on the left and two on the right) point to results labeled Eq 6, Eq 5, Eq 4, and Eq 7. These data should be compared directly to the numbers in the output of Table 2, so as to verify a match to the final decimal place. The column data labeled Eq 4, and Eq 7, in particular, represent the outcome of the circuit analysis. The fact of a verified match confirms that the circuit of Fig. 4 represents the electrical equivalent of the model proposed in ARL-TR-8979.

The circuit components (11, 21, and 31) associated with material species 1 are treated in the leftward columns, those (22, 32) associated with species 2 in the middle columns, and those (33) with species 3 in the rightward columns. For each ij component, values of κ_j , A_i , and L_{ij} are calculated. From these, additional values of R_{ij} and G_{ij} are derived. The voltage divider $.csv_{ij}/\mathcal{V}$ is also calculated for the component, based on the component resistances along the particular pathway channel. From this, the component power consumption normalized by the square of the overall cross-cell voltage drop, P_{ij}/\mathcal{V}^2 , is also derived. Columns, rightward of the component calculations, aggregate the results on a per-channel basis and, moving yet further right, on a network basis, where the equivalent mixed-cell conductivity can be found.

Below the pathway-channel calculation rows in the spreadsheet are the power-consumption calculations, done on a per-species basis. Remember, the given material species may be part of multiple electrical channels—thus, for each species j , we sum the P_{ij}/\mathcal{V}^2 column, while normalizing by the cell volume Ω and converting cross-cell voltage drop \mathcal{V} back to electric-field magnitude E . Comparable calculations for the volume and harmonic averages are provided for comparison below that.

The aggregated output of the present model (mixed-cell conductivity and joule-heating distribution among the mixed-cell species) is highlighted in a mustard color. The values for the volume- and harmonic-averaged approaches are also highlighted in a more faded mustard color, for direct comparison. The observed numerical equivalence, for each respective model, of the conductivity κ and the total power

consumption $P/(\Omega E^2)$ is a check that confirms the validity of Eq. 7, independent of conductivity averaging scheme—namely, that the joule heating per unit volume is proportional to the effective conductivity of the mixed cell. An extracted summary of the spreadsheet is given in Table 4.

Table 4 Summary of results presented in Table 3

	Species 1		Species 2		Species 3		Net
κ_j	1.0		0.8		0.1		0.84831
v_j	0.4		0.4		0.2		1.0
joule heating	$\frac{P_1}{\Omega E^2}$	(%)	$\frac{P_2}{\Omega E^2}$	(%)	$\frac{P_3}{\Omega E^2}$	(%)	$\frac{P}{\Omega E^2} = \kappa_0$
ARL-TR-8979	0.37866	(44.89)	0.44401	(52.63)	0.02093	(2.48)	0.84361
Volume-Avg	0.4	(54.05)	0.32	(43.24)	0.02	(2.70)	0.74
Harmonic-Avg	0.04756	(13.79)	0.05945	(17.24)	0.23781	(68.97)	0.34483

Things that are worthy of note include the following:

- The present model (AR-TR-8979) carries power most efficiently through the species and channel that bring the cumulative volume fraction past the connectivity threshold (species 2 on channel 2 in this example).
- Volume average tries to concentrate joule heating in the most-conductive species.
- Harmonic average tries to concentrate joule heating in the least-conductive species.
- Volume averaged power consumption (always) exceeds the harmonic average.

5.2 Example: Balanced Species Distribution

At this point, we examine other cases of interest. We revise the spreadsheet to include the more recently developed 3-D cubic lattice connectivity functions, $F(f)$, as seen in Table 5. These data are drawn from the Appendix of ARL-MR-1030,⁵ but calculated with greater precision.

In this example, we distribute our three species equally (33%/34%/33%). We choose two orders of magnitude difference between $\kappa_1 = 1$ and $\kappa_3 = 0.01$, with $\kappa_2 = 0.1$ in the logarithmic middle, 1 order of magnitude from the extrema. The data were entered into the revised spreadsheet and a summary of the result is shown in Table 6. The full spreadsheet result is found in Table 7. We note the following points of interest in the summary:

- The volume average and harmonic average are symmetrically mirrored in the percentages of joule heating in the three species, 90/9/1 versus 1/9/90.

Table 5 The $F(f)$ function used for subsequent examples, corresponding to a $5 \times 5 \times 5$ cubic 3-D lattice

5x5x5 F(f) interpolation			
f		F	
0.00E+00	0.0000E+00	5.00E-01	7.2799E-01
2.50E-02	4.8179E-15	5.25E-01	7.9202E-01
5.00E-02	1.3865E-11	5.50E-01	8.3940E-01
7.50E-02	1.5434E-09	5.75E-01	8.7507E-01
1.00E-01	4.4626E-08	6.00E-01	9.0256E-01
1.25E-01	6.1242E-07	6.25E-01	9.2415E-01
1.50E-01	5.2273E-06	6.50E-01	9.4132E-01
1.75E-01	3.2070E-05	6.75E-01	9.5505E-01
2.00E-01	1.5415E-04	7.00E-01	9.6602E-01
2.25E-01	6.1331E-04	7.25E-01	9.7476E-01
2.50E-01	2.0939E-03	7.50E-01	9.8165E-01
2.75E-01	6.2798E-03	7.75E-01	9.8701E-01
3.00E-01	1.6773E-02	8.00E-01	9.9112E-01
3.25E-01	4.0113E-02	8.25E-01	9.9419E-01
3.50E-01	8.5720E-02	8.50E-01	9.9642E-01
3.75E-01	1.6260E-01	8.75E-01	9.9796E-01
4.00E-01	2.7208E-01	9.00E-01	9.9897E-01
4.25E-01	4.0197E-01	9.25E-01	9.9957E-01
4.50E-01	5.3107E-01	9.50E-01	9.9987E-01
4.75E-01	6.4183E-01	9.75E-01	9.9998E-01
		1.00E+00	1.0000E+00

- There is a factor of 13 difference in total joule heating between the volume and harmonic averages.
- The present model (ARL-TR-8979) is the only averaging scheme that focuses joule heating in species 2, which is the material whose cumulative volume fraction (*i.e.*, $v_1 + v_2$) crosses the F threshold.
- In comparison to a cell of pure species 2, in which $P_2/(\Omega_2 E^2) = 0.1$, in this scenario, $P_2/(\Omega_2 E^2) = 0.14798/0.34 = 0.435$, a factor of $4.4 \times$ higher.
- The least-conductive species 3 dissipates $21 \times$ less energy in the present model than in the harmonic model, even though the present model dissipates nearly $8 \times$ the overall energy, in comparison.

Table 6 Summary of results presented in Table 7

	Species 1		Species 2		Species 3		Net
κ_j	1.0		0.1		0.01		0.21275
v_j	0.33		0.34		0.33		1.00
joule heating	$\frac{P_1}{\Omega E^2}$	(%)	$\frac{P_2}{\Omega E^2}$	(%)	$\frac{P_3}{\Omega E^2}$	(%)	$\frac{P}{\Omega E^2} = \kappa_0$
ARL-TR-8979	0.06360	(29.89)	0.14798	(69.56)	0.00117	(0.55)	0.21275
Volume-Avg	0.33	(89.84)	0.034	(9.26)	0.0033	(0.90)	0.3673
Harmonic-Avg	0.00024	(0.90)	0.00252	(9.26)	0.02446	(89.84)	0.02723

5.3 Example: Predominant Greater-Conducting Component

In this example, while we retain the same species conductivities as in the prior example, here we distribute the volume fractions of our three species to favor the most-conductive component (75%/10%/15%). The data were entered into the revised spreadsheet and a summary of the result is shown in Table 8. The full spreadsheet result is found in Table 9. We note the following points of interest in the summary:

- There is a factor of approximately 13 difference in total joule heating between the volume and harmonic averages.
- Because the volume fraction of species 1 is sufficient to cross the F function threshold by itself, the present model (ARL-TR-8979) is highly efficient at establishing pathways exclusively through species 1, even though the volume fraction is merely 75%. Thus, the net conductivity of the mixed cell is 99% of that of species 1. Likewise, 99.5% of the joule heating occurs in species 1.
- In comparison to a cell of pure species 1, in which $P_1/(\Omega_1 E^2) = 1.0$, in this scenario, $P_1/(\Omega_1 E^2) = 0.98473/0.75 = 1.313$, a factor of 1.3× higher.
- The least-conductive species 3 dissipates nearly 8× less energy in the present model than in the volume-average model, even though the present model dissipates nearly 1.3× the overall energy, in comparison.
- The least-conductive species 3 dissipates 281× less energy in the present model than in the harmonic model, even though the present model dissipates nearly 16× the overall energy, in comparison.

Table 8 Summary of results presented in Table 9

	Species 1	Species 2	Species 3	Net
κ_j	1.0	0.1	0.01	0.98904
v_j	0.75	0.10	0.15	1.00
joule heating	$\frac{P_1}{\Omega E^2}$ (%)	$\frac{P_2}{\Omega E^2}$ (%)	$\frac{P_3}{\Omega E^2}$ (%)	$\frac{P}{\Omega E^2} = \kappa_0$
ARL-TR-8979	0.98473 (99.56)	0.00411 (0.42)	0.00019 (0.02)	0.98904
Volume-Avg	0.75 (98.49)	0.01 (1.31)	0.0015 (0.20)	0.7615
Harmonic-Avg	0.00267 (4.48)	0.00356 (5.97)	0.05346 (89.55)	0.0597

5.4 Example: Predominant Lesser-Conducting Component

In this example, while we retain the same species conductivities as in the prior example, here we distribute the volume fractions of our three species to favor the least-conductive component (15%/10%/75%). The data were entered into the revised spreadsheet and a summary of the result is shown in Table 10. The full spreadsheet result is found in Table 11. We note the following points of interest in the summary:

- There is a factor of approximately 13 difference in total joule heating between the volume and harmonic averages.
- Because the combined volume fractions of species 1 and 2 are not sufficient to cross the F function threshold by themselves, the present model (ARL-TR-8979) must rely largely on pathways including all species (*i.e.*, channel 3). Thus, the net conductivity of the mixed cell is roughly equivalent to the harmonic average. As a result, 95.2% of the joule heating occurs in species 3.
- In comparison to a cell of pure species 3, in which $P_3/(\Omega_3 E^2) = 0.01$, in this scenario, $P_3/(\Omega_3 E^2) = 0.01291/0.75 = .0172$, a factor of 1.7 \times higher.
- The conducting species 1 dissipates 1667 \times less energy in the present model than in the volume-average model.

Table 10 Summary of results presented in Table 11

	Species 1		Species 2		Species 3		Net
κ_j	1.0		0.1		0.01		0.01356
v_j	0.15		0.10		0.75		1.00
joule heating	$\frac{P_1}{\Omega E^2}$	(%)	$\frac{P_2}{\Omega E^2}$	(%)	$\frac{P_3}{\Omega E^2}$	(%)	$\frac{P}{\Omega E^2} = \kappa_0$
ARL-TR-8979	0.00009	(0.67)	0.00057	(4.18)	0.01291	(95.15)	0.01356
Volume-Avg	0.15	(89.55)	0.01	(5.97)	0.0075	(4.48)	0.1675
Harmonic-Avg	0.000026	(0.2)	0.00017	(1.31)	0.01293	(98.49)	0.01313

Table 11 Equivalent mixed-cell circuit, with $\kappa_1 = 1$ (15%), $\kappa_2 = 0.1$ (10%), and $\kappa_3 = 0.01$ (75%)

INPUTS	Material1 (is part of Paths 1,2,3)	Material2 (is part of Paths 2,3)	Material3 (is part of Path 3)	per Channel Aggregate	Network Aggregate
k_j	1	0.1	0.01		
v_j	0.15	0.1	0.75		
$f = \sum v_j$	0.15	0.25	1		
$F(f) =$	0.00	0.00	1.00		
Ref: ARL-TR-8979	j=Circuit component composed of Mat. j				
Eq6	$i=A_0$	$i=A_0$	$i=A_0$		
\downarrow	A_1	A_1	A_1		
\downarrow	A_2	A_2	A_2		
\downarrow	A_3	A_3	A_3		
\downarrow	A_4	A_4	A_4		
\downarrow	A_5	A_5	A_5		
\downarrow	A_6	A_6	A_6		
\downarrow	A_7	A_7	A_7		
\downarrow	A_8	A_8	A_8		
\downarrow	A_9	A_9	A_9		
\downarrow	A_{10}	A_{10}	A_{10}		
\downarrow	A_{11}	A_{11}	A_{11}		
\downarrow	A_{12}	A_{12}	A_{12}		
\downarrow	A_{13}	A_{13}	A_{13}		
\downarrow	A_{14}	A_{14}	A_{14}		
\downarrow	A_{15}	A_{15}	A_{15}		
\downarrow	A_{16}	A_{16}	A_{16}		
\downarrow	A_{17}	A_{17}	A_{17}		
\downarrow	A_{18}	A_{18}	A_{18}		
\downarrow	A_{19}	A_{19}	A_{19}		
\downarrow	A_{20}	A_{20}	A_{20}		
\downarrow	A_{21}	A_{21}	A_{21}		
\downarrow	A_{22}	A_{22}	A_{22}		
\downarrow	A_{23}	A_{23}	A_{23}		
\downarrow	A_{24}	A_{24}	A_{24}		
\downarrow	A_{25}	A_{25}	A_{25}		
\downarrow	A_{26}	A_{26}	A_{26}		
\downarrow	A_{27}	A_{27}	A_{27}		
\downarrow	A_{28}	A_{28}	A_{28}		
\downarrow	A_{29}	A_{29}	A_{29}		
\downarrow	A_{30}	A_{30}	A_{30}		
\downarrow	A_{31}	A_{31}	A_{31}		
\downarrow	A_{32}	A_{32}	A_{32}		
\downarrow	A_{33}	A_{33}	A_{33}		
\downarrow	A_{34}	A_{34}	A_{34}		
\downarrow	A_{35}	A_{35}	A_{35}		
\downarrow	A_{36}	A_{36}	A_{36}		
\downarrow	A_{37}	A_{37}	A_{37}		
\downarrow	A_{38}	A_{38}	A_{38}		
\downarrow	A_{39}	A_{39}	A_{39}		
\downarrow	A_{40}	A_{40}	A_{40}		
\downarrow	A_{41}	A_{41}	A_{41}		
\downarrow	A_{42}	A_{42}	A_{42}		
\downarrow	A_{43}	A_{43}	A_{43}		
\downarrow	A_{44}	A_{44}	A_{44}		
\downarrow	A_{45}	A_{45}	A_{45}		
\downarrow	A_{46}	A_{46}	A_{46}		
\downarrow	A_{47}	A_{47}	A_{47}		
\downarrow	A_{48}	A_{48}	A_{48}		
\downarrow	A_{49}	A_{49}	A_{49}		
\downarrow	A_{50}	A_{50}	A_{50}		
\downarrow	A_{51}	A_{51}	A_{51}		
\downarrow	A_{52}	A_{52}	A_{52}		
\downarrow	A_{53}	A_{53}	A_{53}		
\downarrow	A_{54}	A_{54}	A_{54}		
\downarrow	A_{55}	A_{55}	A_{55}		
\downarrow	A_{56}	A_{56}	A_{56}		
\downarrow	A_{57}	A_{57}	A_{57}		
\downarrow	A_{58}	A_{58}	A_{58}		
\downarrow	A_{59}	A_{59}	A_{59}		
\downarrow	A_{60}	A_{60}	A_{60}		
\downarrow	A_{61}	A_{61}	A_{61}		
\downarrow	A_{62}	A_{62}	A_{62}		
\downarrow	A_{63}	A_{63}	A_{63}		
\downarrow	A_{64}	A_{64}	A_{64}		
\downarrow	A_{65}	A_{65}	A_{65}		
\downarrow	A_{66}	A_{66}	A_{66}		
\downarrow	A_{67}	A_{67}	A_{67}		
\downarrow	A_{68}	A_{68}	A_{68}		
\downarrow	A_{69}	A_{69}	A_{69}		
\downarrow	A_{70}	A_{70}	A_{70}		
\downarrow	A_{71}	A_{71}	A_{71}		
\downarrow	A_{72}	A_{72}	A_{72}		
\downarrow	A_{73}	A_{73}	A_{73}		
\downarrow	A_{74}	A_{74}	A_{74}		
\downarrow	A_{75}	A_{75}	A_{75}		
\downarrow	A_{76}	A_{76}	A_{76}		
\downarrow	A_{77}	A_{77}	A_{77}		
\downarrow	A_{78}	A_{78}	A_{78}		
\downarrow	A_{79}	A_{79}	A_{79}		
\downarrow	A_{80}	A_{80}	A_{80}		
\downarrow	A_{81}	A_{81}	A_{81}		
\downarrow	A_{82}	A_{82}	A_{82}		
\downarrow	A_{83}	A_{83}	A_{83}		
\downarrow	A_{84}	A_{84}	A_{84}		
\downarrow	A_{85}	A_{85}	A_{85}		
\downarrow	A_{86}	A_{86}	A_{86}		
\downarrow	A_{87}	A_{87}	A_{87}		
\downarrow	A_{88}	A_{88}	A_{88}		
\downarrow	A_{89}	A_{89}	A_{89}		
\downarrow	A_{90}	A_{90}	A_{90}		
\downarrow	A_{91}	A_{91}	A_{91}		
\downarrow	A_{92}	A_{92}	A_{92}		
\downarrow	A_{93}	A_{93}	A_{93}		
\downarrow	A_{94}	A_{94}	A_{94}		
\downarrow	A_{95}	A_{95}	A_{95}		
\downarrow	A_{96}	A_{96}	A_{96}		
\downarrow	A_{97}	A_{97}	A_{97}		
\downarrow	A_{98}	A_{98}	A_{98}		
\downarrow	A_{99}	A_{99}	A_{99}		
\downarrow	A_{100}	A_{100}	A_{100}		
\downarrow	A_{101}	A_{101}	A_{101}		
\downarrow	A_{102}	A_{102}	A_{102}		
\downarrow	A_{103}	A_{103}	A_{103}		
\downarrow	A_{104}	A_{104}	A_{104}		
\downarrow	A_{105}	A_{105}	A_{105}		
\downarrow	A_{106}	A_{106}	A_{106}		
\downarrow	A_{107}	A_{107}	A_{107}		
\downarrow	A_{108}	A_{108}	A_{108}		
\downarrow	A_{109}	A_{109}	A_{109}		
\downarrow	A_{110}	A_{110}	A_{110}		
\downarrow	A_{111}	A_{111}	A_{111}		
\downarrow	A_{112}	A_{112}	A_{112}		
\downarrow	A_{113}	A_{113}	A_{113}		
\downarrow	A_{114}	A_{114}	A_{114}		
\downarrow	A_{115}	A_{115}	A_{115}		
\downarrow	A_{116}	A_{116}	A_{116}		
\downarrow	A_{117}	A_{117}	A_{117}		
\downarrow	A_{118}	A_{118}	A_{118}		
\downarrow	A_{119}	A_{119}	A_{119}		
\downarrow	A_{120}	A_{120}	A_{120}		
\downarrow	A_{121}	A_{121}	A_{121}		
\downarrow	A_{122}	A_{122}	A_{122}		
\downarrow	A_{123}	A_{123}	A_{123}		
\downarrow	A_{124}	A_{124}	A_{124}		
\downarrow	A_{125}	A_{125}	A_{125}		
\downarrow	A_{126}	A_{126}	A_{126}		
\downarrow	A_{127}	A_{127}	A_{127}		
\downarrow	A_{128}	A_{128}	A_{128}		
\downarrow	A_{129}	A_{129}	A_{129}		
\downarrow	A_{130}	A_{130}	A_{130}		
\downarrow	A_{131}	A_{131}	A_{131}		
\downarrow	A_{132}	A_{132}	A_{132}		
\downarrow	A_{133}	A_{133}	A_{133}		
\downarrow	A_{134}	A_{134}	A_{134}		
\downarrow	A_{135}	A_{135}	A_{135}		
\downarrow	A_{136}	A_{136}	A_{136}		
\downarrow	A_{137}	A_{137}	A_{137}		
\downarrow	A_{138}	A_{138}	A_{138}		
\downarrow	A_{139}	A_{139}	A_{139}		
\downarrow	A_{140}	A_{140}	A_{140}		
\downarrow	A_{141}	A_{141}	A_{141}		
\downarrow	A_{142}	A_{142}	A_{142}		
\downarrow	A_{143}	A_{143}	A_{143}		
\downarrow	A_{144}	A_{144}	A_{144}		
\downarrow	A_{145}	A_{145}	A_{145}		
\downarrow	A_{146}	A_{146}	A_{146}		
\downarrow	A_{147}	A_{147}	A_{147}		
\downarrow	A_{148}	A_{148}	A_{148}		
\downarrow	A_{149}	A_{149}	A_{149}		
\downarrow	A_{150}	A_{150}	A_{150}		
\downarrow	A_{151}	A_{151}	A_{151}		
\downarrow	A_{152}	A_{152}	A_{152}		
\downarrow	A_{153}	A_{153}	A_{153}		
\downarrow	A_{154}	A_{154}	A_{154}		
\downarrow	A_{155}	A_{155}	A_{155}		
\downarrow	A_{156}	A_{156}	A_{156}		
\downarrow	A_{157}	A_{157}	A_{157}		
\downarrow	A_{158}	A_{158}	A_{158}		
\downarrow	A_{159}	A_{159}	A_{159}		
\downarrow	A_{160}	A_{160}	A_{160}		
\downarrow	A_{161}	A_{161}	A_{161}		
\downarrow	A_{162}	A_{162}	A_{162}		
\downarrow	A_{163}	A_{163}	A_{163}		
\downarrow	A_{164}	A_{164}	A_{164}		
\downarrow	A_{165}	A_{165}	A_{165}		
\downarrow	A_{166}	A_{166}	A_{166}		
\downarrow	A_{167}	A_{167}	A_{167}		
\downarrow	A_{168}	A_{168}	A_{168}		
\downarrow	A_{169}	A_{169}	A_{169}		
\downarrow	A_{170}	A_{170}	A_{170}		
\downarrow	A_{171}	A_{171}	A_{171}	</	

5.5 Overall Comparison of the Conductivity-Averaging Schemes

In looking at the results of the prior examples studied in this report, a certain picture emerges about the conductivity model of ARL-TR-8979 with respect to the volume- and harmonic-averaged models. This uniqueness applies in regard to both conductivity and joule heating.

5.5.1 Conductivity

With the volume-averaged model, the most-conductive species in the mixed cell tends to drive the net conductivity. For example, in Table 10, the volume-averaged model exhibits behavior in which the net conductivity is larger than the species conductivity of 85% of the material in the cell. That is to say, 15% of the κ_1 -material more than balances out the 75% of κ_3 -material in the cell.

In this regard, the harmonic-averaged model is equally extreme in the opposite direction, favoring the properties of the least-conductive component in the mixed cell. In Table 8, we see the net conductivity of the harmonic model falls below that of 85% of the material in the cell. The 15% of the κ_3 -material within the cell is driving the magnitude of the overall conductivity. This effect would be even greater if the range of conductivities in the cell were larger than the 2 orders of magnitude considered in our examples.

In contrast to these two extremes, the present model of ARL-TR-8979 exhibits a blend of these behaviors. When the volume fractions of mixed-cell species favors the most-conductive species, this model presents a net conductivity that favors conduction. When the volume fractions favor the least-conductive species, the net conductivity provided by this model is in line with that species.

A reaffirming trend with this behavior is that a small volume fraction of contaminant in a cell does little to change the overall conductivity of the cell, unlike the volume-average model, which changes conductivity in proportion to the fraction of contaminant, and the harmonic-average model, which works to favor the least-conductive material, regardless of whether it is the primary material or the contaminant.

5.5.2 Joule Heating

The distribution of joule heating for the various averaging schemes is, if anything, even more telling than the conductivity calculation. In the volume-average approach,

as the volume fraction of the most-conductive species 1 was varied from 15% to 75% in the examples, the percentage of joule heating concentrated in species 1 never falls below 89.5% of the total.

In the same manner, with the harmonic-average approach, as the volume fraction of the least-conductive species 3 was varied from 15% to 75% in the examples, the percentage of joule heating concentrated in species 3 never falls below 89.5% of the total.

The mirror symmetry of these two models is no accident, given that one is a purely parallel circuit and the other purely serial. In the parallel circuit, voltage drop is equal across all components and the current is proportional to the component conductance. In the serial circuit, the current through all components is equal and the voltage drop is proportional to the component resistance. Since power consumption is $P = \mathcal{V}i = \mathcal{V}^2G = i^2R$ and $G = 1/R$, it follows that \mathcal{V}^2G for the components of the parallel circuit looks functionally like i^2R for the components of the serial circuit.

In contrast to these two archetypal circuit layouts, the present model exhibits properties of both parallel and serial circuits, as seen in Fig. 4. When there is ample supply of high-conductivity species 1 in the mixed cell, enough electrical pathways can establish themselves through species 1 so that $A_1 > A_2 > A_3$ and the circuit is functionally parallel. But if the quantity of species 1 and 2 is small in the mixed cell, the areas A_1 and A_2 become small, indicating that large numbers of connections could not manifest across the cell using only those two species. Thus, in this case, the predominant path of the circuit belongs to channel 3, which embodies all the mixed-cell species arranged in serial.

In the present model, the transition from serial to parallel behavior and vice versa is governed by the F -function threshold. In particular, starting with the most-conductive species, the question of “how many species are required to reach the total-volume fraction corresponding to the F -function threshold value?” becomes the key question. If it takes k species of the n total in the cell to pass that threshold, then channel k will comprise the predominant pathways in the circuit, consisting of species 1, ..., k .

To see this in action, we need merely look at the prior examples. In the first example (see Table 7), with an equal partition of species in the cell, we note that it is species

2 that takes the cumulative volume across the F -function threshold. Thus, from the table, we see that channel 2 comprises $A_2 = 90.3\%$ of the total pathways, while A_1 only comprises 4.9% of such pathways. While channel 1 will dissipate energy exclusively in species 1, channel 2 dissipates in both species 1 and 2. However, because the resistivity of species 2 is a factor of 10 times that of species 1, the vast majority of dissipation along channel 2 occurs in species 2. Overall, 69.56% of joule heating occurs in species 2 and only 29.89% in species 1 (the remaining 0.55% in species 3).

In example 2 (see Table 9), the volume fraction of species 1 (75%) is sufficient to push past the F -function threshold by itself. Thus, channel 1, comprising solely species 1, provides connectivity for $A_1 = 98.2\%$ of the mixed-cell circuit pathways. Not surprisingly, therefore, 99.6% of the joule heating also occurs in species 1.

In example 3, the situation is reversed. The species 1 and 2 only compose 25% of the mixed cell, which is not sufficient to cross the conductivity threshold. Thus, it falls upon channel 3 to establish the vast majority of pathways across the cell. Because this channel is a serial circuit comprising all three materials in the cell, the net result should be very similar to the harmonic average. This proves to be the case, with over 98% of the pathways in channel 3. Correspondingly, 95.2% of joule heating occurs in species 3 (similar to the 98.5% for the harmonic-averaged approach).

6. Possible Inconsistencies for Further Study

The big advantage of being able to cast the conductivity-averaging scheme in terms of an equivalent circuit is that it permits a clearer understanding of the model and how its components interact. It is, therefore, also capable of highlighting model inconsistencies that may indicate negative features of the scheme. In this regard, there are two features of the model of ARL-TR-8979¹ that warrant further consideration.

First, the calculation of channel cross sections, originally embodied in the terms $F_{1\cap\dots\cap j}$ and $F_{1\cup\dots\cup j}$, now also described by Eq. 13,* allows for a channel cross section that is larger than the cross section of the physical material available in those species. While it is wholly consistent, for example, that the introduction of porosity into a material could lower the effective conducting cross section of the specimen,

*To draw fully the connection in nomenclature between the model notation of ARL-TR-8979 and Eq. 13, it is the case that $A_i/A_0 = F_{1\cap\dots\cap j}$, where $i = j$.

Eq. 13 also allows for the possibility that significant porosity could be introduced without reducing the effective conducting cross-sectional area. Such a possibility seems counterintuitive and therefore needs to be revisited.

A second model facet of ARL-TR-8979 that is worthy of further study concerns the explicitly stated assertion that a physical material point in the mixed cell may be part of several distinct electrical channels. This point is manifested in Eq. 12, in which the amount of a material species available to construct channel pathways is undiminished, regardless of usage along other channels. This formulation has the net effect of making the volume fractions of material used in the equivalent circuit different from the volume fractions in the actual mixed cell and always favoring the more conductive species. Whether such species *overutilization* has a physical basis requires further consideration.

Because the intent of this report is to introduce the notion of equivalent sub-circuits for the various mixed-cell conductivity-averaging schemes, we do not address in this report the validity of these modeling concerns. Suffice it here to say that such concerns only arose because of the increased understanding provided by the equivalent circuits developed for this report. We will leave it to a future study to address these concerns.

7. Conclusion

In this report, we examine three approaches to treating the conductivity of a mixed computational cell: the volume-average approach, the harmonic-average approach, and the present approach detailed originally in ARL-TR-8979.¹ The ability to create equivalent sub-circuits corresponding to each of these approaches was demonstrated by virtue of the fact that, in each case, the circuit conductivity could be shown to be identical to the mixed-cell conductivity of the associated scheme.

The ability to characterize each mixed-cell conductivity model as an equivalent sub-circuit is a strategically important advance! Because the analysis of circuits is a well-established engineering discipline, the equivalent sub-circuit not only yields up an equivalent conductivity, but also the distribution of joule heating among the various “components” of the circuit. These “components” represent material along resistive pathways of conduction in the mixed cell. Therefore, the joule heating of the sub-circuit components provides a direct measure of the joule-heating distribution

among each of the mixed-cell species, which is a key item of required understanding for any conductivity-averaging scheme.

The volume-averaging approach to conductivity was shown equivalent to a parallel sub-circuit of n channels, where each channel of the sub-circuit is occupied by one of the n material species in the mixed cell. While the length of each channel is the length of the cell, the cross section of the channel is proportional to the volume fraction of the respective species that constitutes it.

In the case of the harmonic-averaging approach to conductivity, the equivalent sub-circuit is a serial circuit, comprising elements made up from each of the n species in the mixed cell. The cross section of each component is the mixed-cell cross section, while the length of each component is in proportion to the volume fraction of the species constituting the element.

Like the volume-averaged model, the present model (introduced in ARL-TR-8979) produces an equivalent sub-circuit of n channels. However, unlike volume averaging, the channels can comprise more than a single resistive component. The first channel comprises one component, the second two components, and so on until the n th channel. Of these $n(n + 1)/2$ components, n are composed of the most-conductive species-1, $n - 1$ are composed of species-2, and so on. Section 4 of this report should be consulted to understand the manner in which the resistive values for each of these components is calculated and the layout by which they are arranged. However, a key point is that this sub-circuit design can exhibit both parallel and serial behavior, depending on the particular volume-fraction distribution of the species in the mixed cell.

We see, in the examples presented in this report, the ability of the present model to adjust to a serial or parallel nature for the mixed-cell sub-circuit, on the basis of the volume fractions of the constituents. Logically, a mixed cell in which the conducting element predominates will tend to parallel-circuit behavior, as there will exist many pathways that can proceed exclusively through this most-conductive species. In contrast, a mixed cell in which the less-conductive species predominates will tend toward serial-circuit behavior, since this species is necessary to establish connectivity while at the same time pathways will attempt to serially divert into the more-conductive species when presented with the topological opportunity. The

present model is the only one of the three studied that permits this contextual switch automatically.

The development of an equivalent circuit corresponding to each of the averaging schemes considered in this report provides a clearer picture of the model principles. This feature helps in evaluating the tenets of each model, both for consistency and accuracy. For the model of ARL-TR-8979, the circuit highlights two possible inconsistencies that should be examined in a future study. In this regard, the introduction of model-equivalent sub-circuits is already helping to spur future improvements for mixed-cell conductivity-averaging schemes.

8. References

1. Segletes S. A model for the electrical conductivity of a mixed computational cell. DEVCOM Army Research Laboratory; 2020 June. Report No.: ARL-TR-8979.
2. Siefert C, Sandia National Laboratories. Personal communication, 2021 Mar 4 (Joule Heating in ALEGRA. 2016 Aug 10).
3. Niederhaus J, Sandia National Laboratories. Personal communication, 2020 Oct 23 (Siefert, C. Mixed Material Models for Poisson. 2020 Aug 20).
4. Segletes S. On the electrical connectivity of a 2-D, randomly distributed, two-component (conducting/insulating) mixture. DEVCOM Army Research Laboratory; 2020 Jan. Report No.: ARL-TR-8899.
5. Segletes S. An examination of connectivity across 3-D cubic-lattice networks. DEVCOM Army Research Laboratory; 2021 Feb. Report No.: ARL-MR-1030.

1 (PDF)	DEFENSE TECHNICAL INFORMATION CTR DTIC OCA	FCDD RLW W W OBERLE
1 (PDF)	DEVCOM ARL FCDD RLD DCI TECH LIB	FCDD RLW WA K MCNESBY FCDD RLW WB B ROOS FCDD RLW MB B LOVE G GAZONAS
1 (PDF)	COMMANDER US ARMY AVN & MISSILE CMD S CORNELIUS	FCDD RLW MC R JENSEN
1 (PDF)	NSWC INDIAN HEAD DIVISION T P MCGRATH II	FCDD RLW MD S WALSH FCDD RLW ME P PATEL
1 (PDF)	NAVAIR E SIEVEKA	FCDD RLW T R FRANCAERT J HOGGE T VONG R YEAGER
1 (PDF)	US ARMY ERDEC J Q EHRGOTT JR	FCDD RLW TA S R BILYK P BERNING M COPPINGER J FLENIKEN M J GRAHAM M GREENFIELD W C UHLIG C WOLFE
3 (PDF)	SANDIA NATIONAL LABS J NIEDERHAUS C SIEFERT A E RODRIGUEZ	FCDD RLW TB C HOPPEL S SATAPATHY
1 (PDF)	ATR CORP A WARDLAW	FCDD RLW TC J CAZAMIAS M FERREN-COKER R BECKER D CASEM J CLAYTON B LEAVY J LLOYD S SEGLETES L SHANNAHAN A TONGE C WILLIAMS
1 (PDF)	SOUTHWEST RESEARCH INST T HOLMQUIST	
3 (PDF)	DE TECHNOLOGIES R CICCARELLI W FLIS W CLARK	
1 (PDF)	APPLIED RESEARCH ASSOC INC R T BOCCHIERI	
1 (PDF)	DREXEL UNIVERSITY B FAROUK	
	<u>ABERDEEN PROVING GROUND</u>	
77 (PDF)	DEVCOM ARL FCDD RLD P BAKER FCDD RLD D T ROSENBERGER FCDD RLW S SCHOENFELD FCDD RLW C D LYON	

FCDD RLW TD

A BARD
N BRUCHEY
R DONEY
S HALSEY
M KEELE
D KLEPONIS
F MURPHY
D PETTY
C RANDOW
S SCHRAML
K STOFFEL
G VUNNI
V WAGONER
M ZELLNER

FCDD RLW TE

P SWOBODA
P BARTKOWSKI
D GALLARDY
D HORNBAKER
E HORWATH
J HOUSKAMP
E KLIER
C KRAUTHAUSER
M LOVE
K MCNAB
D SHOWALTER

FCDD RLW TF

T EHLERS
E KENNEDY
L MAGNESS
C MEYER
B SORENSEN
R SUMMERS

FCDD RLW TG

N GNIAZDOWSKI
C CUMMINS
E FIORAVANTE
D FOX
R GUPTA
S HUG
S KUKUCK
C PECORA
J STEWART

FCDD DAS LBE

C BARKER
D HOWLE
FCDD DAS LBG
P MERGLER
J ABELL
P HORTON
FCDD DAS LBS
M PERRY
D LYNCH
J SHINDELL
FCDD DAS LBW
R BOWERS

12
(PDF)

DEVCOM DAC
FCDD DAS LBA
D FORDYCE
FCDD DAS LBD
R GROTE
J POLESNE